Check for updates

Enhancing landfill gas bio-desulfurization: operational insights and microbial dynamics from the Daegu Bangcheon-ri Sanitary Landfill

Eunsue Cho[1,2], Young-Hyun You[3], Chang-Gi Back[4] and Ji Won Hong[2,5]*

[1]Daesung Eco-Energy, Daegu, Republic of Korea, [2]Department of Hydrogen and Renewable Energy, Kyungpook National University, Daegu, Republic of Korea, [3]Species Diversity Research Division, National Institute of Biological Resources, Incheon, Republic of Korea, [4]Department of Environmental Horticulture and Landscape Architecture, Environmental Horticulture, Dankook University, Cheonan, Republic of Korea, [5]Advanced Bio-Resource Research Center, Kyungpook National University, Daegu, Republic of Korea

This study evaluates the efficacy of the Thiopaq bio-desulfurization system at the Daegu Bangcheon-ri Sanitary Landfill in Korea over 1 year focusing on operational insights and microbial dynamics. The system employs sulfur-oxidizing bacteria (SOBs) to convert hydrogen sulfide (H_2S) in landfill gas (LFG) into elemental sulfur. Key findings include maintaining over 96% H_2S removal efficiency despite operational challenges such as sulfur clogging and foam formation. Significant microbial community shifts were observed, with *Thioalkalibacter halophilus* remaining robust, *Alkalilimnicola ehrlichii* declining, and *Halothiobacillus kellyi* becoming more prominent, especially during new well installations with high thiol (methanethiol) concentrations. Scanning electron microscopy revealed distinct morphological characteristics of bio-sulfur under varying conditions contributing to process optimization. Our results underscore the necessity for continuous monitoring and adaptive management of microbial populations and system parameters to effectively handle fluctuating LFG compositions and operational conditions. This study provides substantial guidance for enhancing LFG quality and bio-sulfur production in large-scale landfills.

1 Introduction

In landfills, the degradation of organic waste produces various gases including hydrogen sulfide (H_2S) and other corrosive compounds. These gases pose significant environmental and human health risks and threaten the integrity of landfill infrastructure such as landfill gas (LFG) wells, pipes, and engines used for LFG conversion (Nam et al., 2011). In particular, H_2S is a toxic gas with a characteristic rotten egg smell and can cause respiratory problems and other health issues at high concentrations (Ko et al., 2015; Long et al., 2016). Corrosive gases like H_2S can lead to the deterioration of technical components in landfills (Panza and Belgiorno, 2010). This includes the corrosion of metal parts which can
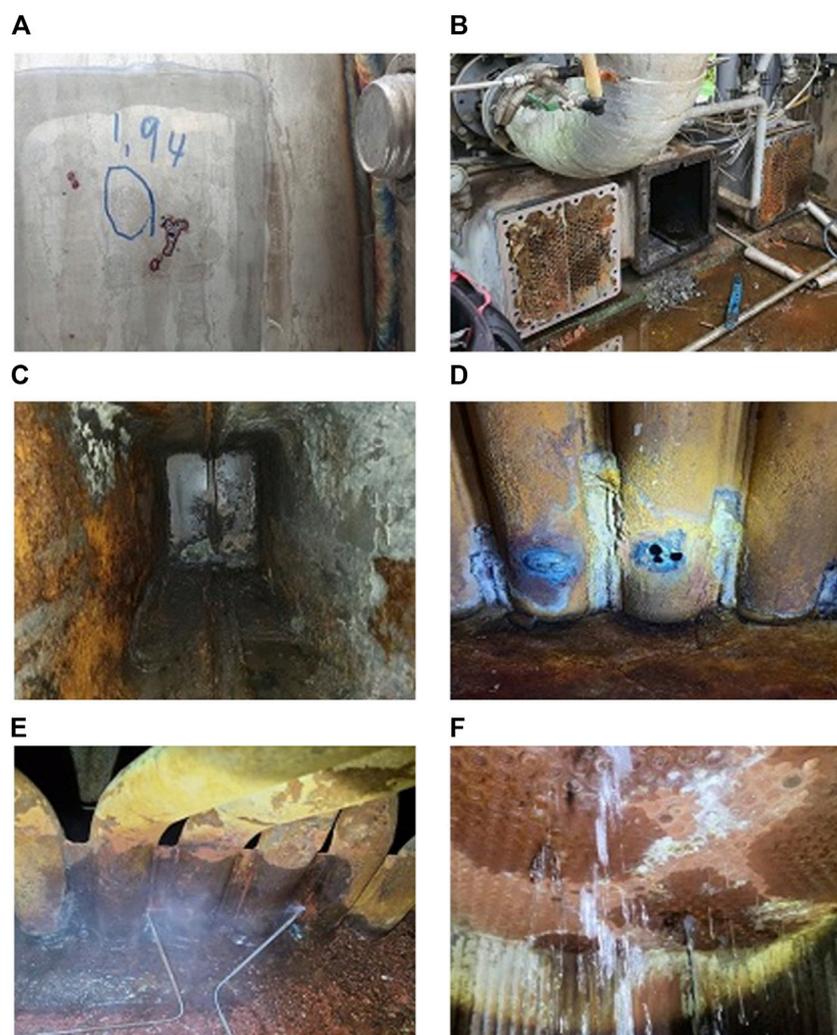
FIGURE 1
H_2S Corrosion damage: **(A−C)** corrosion in the LFG Plant; **(D−F)** corrosion in the HWB.

compromise the structural integrity of LFG collection and conversion systems. Effective abatement techniques are essential to mitigate these impacts and ensure the safe and efficient operation of landfill sites (Wang et al., 2022).

Several methods have been employed to reduce the concentration of H_2S and other corrosive gases in LFG (Toledo-Cervantes et al., 2017). These include physical and chemical adsorption techniques such as activated carbon filters and scrubbers which are commonly used to capture and neutralize the corrosive gases (Vikrant et al., 2018; Georgiadis et al., 2020). However, these methods come with significant cost and maintenance challenges. The initial installation and ongoing operation of these systems are expensive and they require regular maintenance and frequent replacement of adsorption materials adding to the overall operational costs. Additionally, adsorbent materials can become saturated over time reducing their effectiveness and necessitating timely monitoring and replacement to prevent the breakthrough of untreated gases. Chemical treatments such as the addition of iron salts to form insoluble sulfides (Erdirencelebi and Kucukhemek, 2018; Oh et al.,

2024) and biological treatments where specific bacteria oxidize H_2S into less harmful substances (Rujisangvittaya and Phoolphundh, 2015; Hou et al., 2018) offer alternative solutions. By implementing effective biological H_2S abatement techniques, it is possible to protect both the environment and the infrastructure critical to LFG management and energy recovery economically and efficiently at ambient temperature and atmospheric pressure without the need for toxic chemicals (Chen et al., 2021).

The Daegu Bangcheon-ri Sanitary Landfill (DBSL), the second-largest landfill in Korea, was established and has been under the management of Daegu Metropolitan City since 1990. Moreover, a facility for capturing and utilizing LFG, operated by Daesung Eco-Energy, was installed in 2006. A large amount of GHG has been reduced by collecting LFG and converting it into energy at the DBSL site. From 2007 to 2021, the Clean Development Mechanism (CDM) project has been recognized for achieving a reduction of 3,863,026 tons of CO_2 equivalent in GHG emissions. The duration of the CDM project extends until 2026. Despite successful LFG-to-energy projects, challenges arise from the presence of harmful components such as H_2S, ammonia (NH_3),
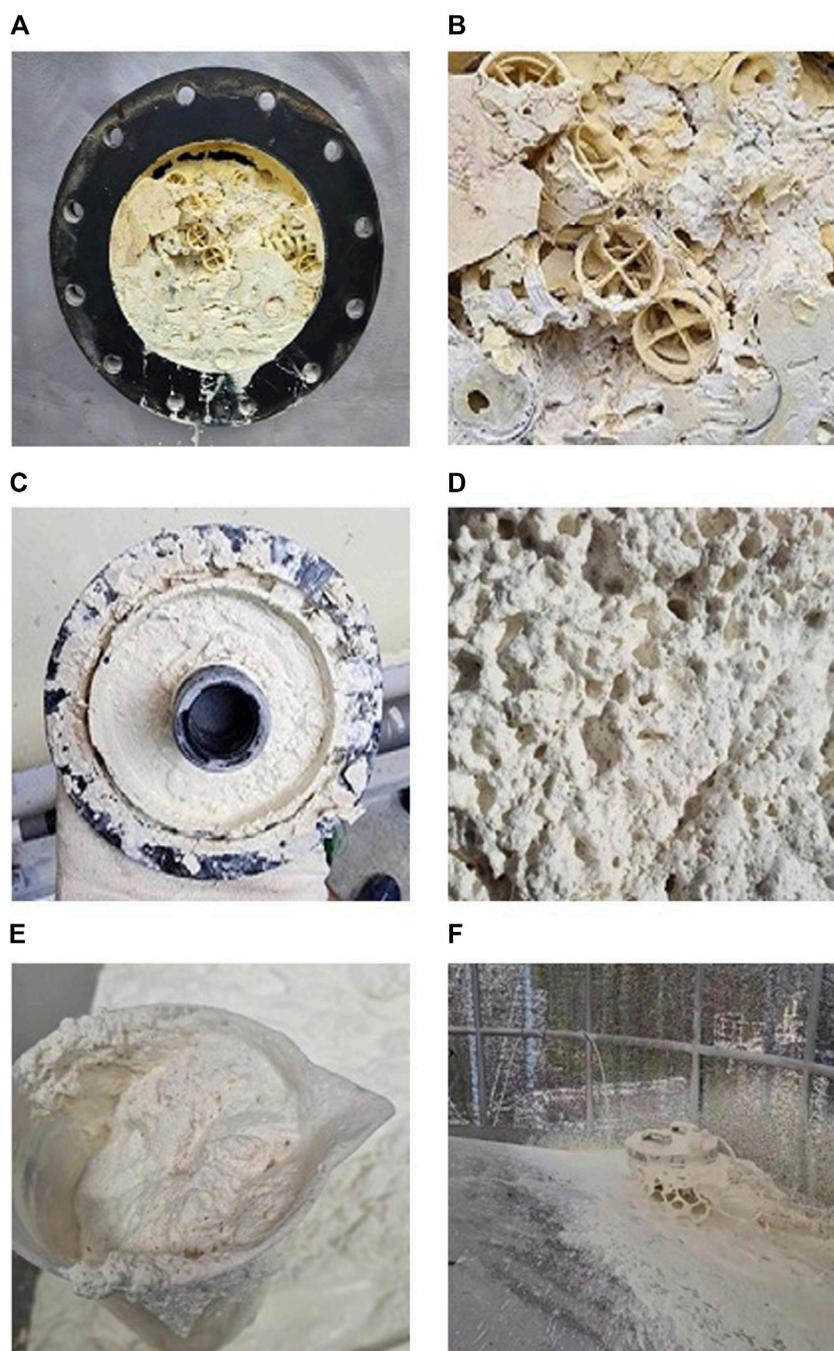
FIGURE 2
Issues in the Thiopaq facility: **(A–C)** sulfur clogging; **(D–F)** rapid foam formation.

and BTEX (benzene, toluene, ethylbenzene, and xylene) in LFG. These substances are known as the major odorants, and trimethylamine and sulfur compounds are the main cause of odor at the DBSL (Jeon, 2014). Among them, H_2S poses a significant environmental and health concern (Plaza et al., 2007). Originating from organic matter, sludge waste, gypsum, and construction debris in landfills, H_2S contributes to foul odors and corrosion challenges (Eun et al., 2007; Plaza et al., 2007; Tolaymat and Carson, 2015). The corrosive impact extends to equipment in LFG plants at the DBSL site (Figures 1A–C). H_2S also causes

significant damage to the hot water boiler (HWB) in facilities utilizing LFG as an energy source (Figures 1D–F). Moreover, with the Korean Government reinforcing the Clean Air Conservation Act (2022) related to sulfur oxide emission, there was a heightened necessity for further advancements in H_2S purification techniques.

To address these challenges, the Thiopaq process, a type of biological desulfurization system, has been implemented. This technology removes H_2S from gaseous streams by absorbing it into a mild alkaline solution and then oxidizing the absorbed

FIGURE 3
Schematic depicting the 16S rRNA gene and the approximate locations of the variable regions (V1-V9) that can be selected for amplicon-based sequencing.

sulfide (HS^-) to elemental sulfur (S^0) with the assistance of naturally occurring microorganisms. Thiopaq process economically and efficiently eliminates H_2S from LFG, offering a sustainable solution with reusable alkaline solutions and natural microorganisms, and producing sulfur biologically (also known as bio-sulfur) as a primary product.

The goal of this research is to enhance the quality and utilization of LFG from large-scale landfills through sulfur-oxidizing bacteria (SOB)-based biological purification techniques, ultimately leading to improved and stable bio-sulfur production. Furthermore, this study aims to provide substantial guidance for future research and practical applications by offering insights into the characteristics of LFG from large-scale landfills and the variations in the SOB community influenced by diverse environmental factors.

2 Materials and methods

2.1 Overview of research project

This 1-year research project, conducted at the DBSL site using the Thiopaq system, aimed to ensure operation stability, protect the facility from corrosion, mitigate odors around the landfill, and ultimately provide a comfortable environment for nearby residents. The study involved analyzing the landfill site environment and LFG characteristics, identifying dominant dominant SOBs species adapted to the DBSL site conditions, species adapted to the DBSL site conditions, and determining other optimal operational factors. However, operational challenges such as sulfur clogging (Figures 2A–C) and rapid foam formation (Figures 2D–F) were encountered. To address these issues, a variety of analyses were conducted on operational data, microbiome changes, water quality, and the surface morphology of bio-sulfur to identify the root causes.

2.2 Landfill site

The DBSL is the only landfill site currently in operation in Daegu, and it handles most of the household waste that is not suitable for recycling or incineration. The DBSL site is located at 820, Dasa-ro, Dasa-eup, Dalseong-gun, Daegu, Korea, and is geographically positioned at N35°52′42″ and E128°30′33″. It is surrounded by mountains on all sides except the north. Daegu has a temperate climate, with an annual average temperature of 14.7°C and an average annual precipitation of 1,022 mm. Daegu Metropolitan City began landfilling waste at the DBSL site in 1990 and plans to continue its use until approximately 2067.

After landfill operations are completed, there are plans to transform the site into an ecological park. The total landfill area covers 853,400 m^2, with a capacity of 32,378,541 m^3.

In Korea, waste is broadly categorized into household and industrial wastes under the Wastes Control Act (2023). Household waste includes all waste types except industrial waste, while industrial waste encompasses industrial general, construction, and designated wastes (including medical waste). The DBSL accepts household waste (excluding food waste), industrial general waste from specific business premises, and bulky waste and incineration ash from waste-to-energy facilities. As of 2023, the waste disposed of at the DBSL site comprised approximately 47% household waste and 53% industrial waste. The composition of the household waste was 17% food waste, 21% paper, 17% wood, 14% textiles, and 31% other materials. Compositional analysis revealed a moisture content of 29%, a combustible fraction of 55%, and a non-combustible fraction of 16%, with a waste density of 0.27 tons/m^3. The calorific value was approximately 2,900 kcal/kg.

From 1990 to 2023, a total of 21,129,361 tons of waste were landfilled at the DBSL site. In the early 1990s, over a million tons of waste were disposed of annually, but this figure has decreased to approximately 300,000 tons annually in the 2020s due to environmental concerns and the implementation of waste-to-energy utilization policies. Furthermore, direct landfilling of household waste will be prohibited from 2030 according to the Enforcement degree of the Waste Control Act (2022); only residues from incinerated household waste or waste-to-energy facilities will be permitted for landfilling which is expected to further reduce the volume of landfill waste.

2.3 LFG plant

The LFG utilization process at DBSL involves capturing, refining, supplying, and utilizing LFG. A vertical collection system was installed at the DBSL site to capture LFG, offering several advantages such as higher LFG capture efficiency and relatively easier maintenance compared to a horizontal system. Currently, there are 213 regular LFG collection wells and 65 temporary collection wells in operation at DBSL. The size of the main pipelines for transporting the collected LFG to the refinery is 400 mm, while the auxiliary pipes are 300 and 200 mm in diameter, respectively.

In the LFG plant, a blower induces negative pressure to draw LFG from the ground at DBSL into the facility. Upon arrival at the LFG plant, the water collected along with the LFG is first removed via a liquid knockout. H_2S is then removed using the Thiopaq system. Following this, the water in the LFG is condensed through a cooler and the condensed water and particles are removed through a

TABLE 1 Production and revenue of LFG at DBSL since 2006.

Year	LFG collection (Nm³/year)	CH$_4$ (%)	Incineration (Nm³/year)	LFG supply to HWB (Nm³/year)	CH$_4$ (%)	Heat value (Gcal)	Revenue (US$[a])
2006	11,289,776	51.30	0	11,394,084	51.98	56,261	1,004,244.8
2007	52,620,878	51.41	51,494	51,243,148	51.78	252,060	4,577,064.4
2008	49,696,622	49.54	0	49,269,712	50.14	234,681	4,861,297.1
2009	47,822,497	49.14	0	47,767,272	49.52	224,697	5,150,223.7
2010	45,194,577	47.57	0	45,475,336	47.96	207,182	4,777,748.6
2011	48,229,724	48.04	0	48,431,596	48.31	222,278	5,096,830.4
2012	44,306,083	48.83	0	44,248,584	48.65	204,519	5,265,272.4
2013	45,839,855	48.72	1,530,716	44,524,452	47.78	198,510	5,500,424.4
2014	46,196,524	48.40	1,280,075	45,061,624	48.08	201,320	5,736,101.1
2015	47,382,397	44.91	2,368,130	45,285,596	44.98	190,542	5,428,961.1
2016	52,204,593	45.03	5,741,400	39,896,116	44.33	194,433	4,577,906.7
2017	51,376,793	47.06	8,492,725	42,970,546	46.77	188,270	4,258,137.8
2018	53,292,565	47.56	18,872,302	34,435,338	46.62	151,297	3,328,744.7
2019	56,891,121	46.97	6,713,201	50,486,876	47.19	225,667	5,049,797.1
2020	55,643,642	43.31	5,069,631	50,802,758	43.46	209,453	4,731,516.9
2021	51,647,956	43.35	11,229,323	40,694,572	43.31	166,697	3,710,356.7
2022	43,793,970	40.60	5,942,806	37,853,636	40.62	145,856	3,663,186.0
2023	38,352,374	46.86	6,347,469	32,024,500	46.75	142,191	4,631,826.9

[a]The exchange rate is calculated as approximately 1,300 kRW, to 1 USD.

TABLE 2 Average H$_2$S concentration levels at the DBSL site.

Year	2008	2009	2010	2011	2012	2013	2014	2015	2016	2017	2018	2019	2020
H$_2$S (ppm)	426	542	622	1,040	948	882	1,416	1,100	1,304	1,488	1,450	3,130	3,300

filter. The refined LFG is stored in a gas holder tank. This stored LFG is supplied to the HWB facility, located 8 km away, to produce heat or is incinerated at the flare stack during low-demand seasons. The facility consistently generates revenue by utilizing a large amount of LFG (Table 1).

In order to measure the H$_2$S concentration, the LFG composition and harmful substances entering the plant are manually measured and recorded at 08:00, 12:00, 16:00, and 20:00 every day through a portable measuring device (Biogas 5000, Geotech, United Kingdom) at the condensate separator of the LFG plant.

There has been an increase in the average H$_2$S concentrations at the DBSL site (Table 2). While initial stages recorded H$_2$S concentrations below 500 ppm, recent years have seen an annual average exceeding 3,000 ppm.

2.4 Thiopaq desulfurization system

The Thiopaq system, a biological desulfurization process, was installed at DBSL in November 2021 to reduce the emission of sulfur

oxides at HWB and to prevent corrosion of the LFG plant. Designed to handle a capacity of 7,000 Nm³/h for LFG flow, the Thiopaq system achieves high efficiency by reducing H$_2$S levels from a maximum of 8,000 to 300 ppm. The system includes a scrubber, bioreactor, and settler with crucial reactions occurring in the scrubber and bioreactor.

The process begins with the absorption of H$_2$S in the scrubber. In this process, H$_2$S is removed from the gas stream by using an alkaline solution with dilute sodium hydroxide (NaOH 25%, OCI, Korea) (Equations 1, 2). The dissolved sulfide is then oxidized to sulfur in the bioreactor. In this step, with the supply of O$_2$, SOBs convert the dissolved sulfide into solid sulfur regenerating OH$^-$ for H$_2$S removal. The solution from the bioreactor is sprayed back into the scrubber reducing the need for NaOH (Equation 3). The formed solid elemental sulfur is then separated from the liquid by sedimentation in the settler (Kleinjan et al., 2003).

$$H_2S(g) \rightarrow H_2S(aq) \tag{1}$$

$$H_2S(aq) + OH^- \rightarrow HS^- + H_2O \tag{2}$$

$$HS^- + \frac{1}{2}O_2 \rightarrow S^0 + OH^- \tag{3}$$
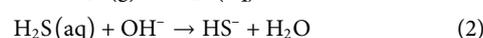
Apart from this, undesirable side reactions can occur. In the scrubber, polythiophosphate ions (S_x^{2-}, with $x \leq 6$) could form due to the reaction of hydrogen sulfide with sulfur (Equation 4). Solid sulfur, which is not completely separated in the settler, is supplied back to the scrubber through liquid recirculation. In the bioreactor, polythiophosphate anions may either decompose into sulfide and sulfur (Equation 5) or be oxidized to thiosulfate (Equation 6). Additionally, sulfate could form through the oxidation of sulfide or sulfur (Equation 7) (Kleinjan et al., 2003).

$$HS^- + (x - 1)S^0 \rightarrow S_x^{2-} + H^+ \qquad (4)$$

$$S_x^{2-} + H^+ \rightarrow HS^- + (x - 1)S^0 \qquad (5)$$

$$S_x^{2-} + \frac{3}{2}O_2 \rightarrow S_2O_3^{2-} + (x - 2)S^0 \qquad (6)$$

$$HS^- + 2O_2 \rightarrow SO_4^{2-} + H^+ \qquad (7)$$
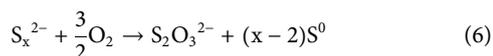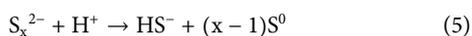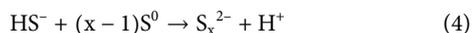
Due to the side reactions forming sulfate and thiosulfate, NaOH has to be continuously injected. To minimize the required amount of NaOH, reducing these undesirable side reactions is essential. Maintaining a low O_2 concentration can prevent the oxidation of sulfide to sulfate. However, controlling the oxidation of anionic polysulfides through oxygen concentration alone is challenging. Additionally, a bleed stream is required to prevent the accumulation of sodium salts due to NaOH injection and nutrient supplementation is also necessary to maintain microbial activity.

LFG entered to the plant was purified through Thiopaq system and outflow H_2S concentration was measured by a spectrometer-type H_2S analyzer (GasEye Cross Duct, Airoptic, Poland). H_2S levels were measured in real time and displayed on the supervisory control and data acquisition (SCADA) system with an alarm function.

2.5 Water quality analysis

Samples from the bioreactor were collected monthly from April 2022 to March 2023 with additional sampling during significant changes. The analysis aimed to evaluate the impact of water quality on microbial diversity and sulfur formation (S^0). Prior to analysis, a filtration process using a 0.22 μm filter (Minisart, Sartorius Stedim Biotech, Germany) was employed to remove microorganisms and organic matter from each sample. After filtration, the solution was diluted 20-fold with 2% nitric acid (Thermo Fisher Scientific, United States). Following pre-treatment, the elemental contents of the samples were quantified using an inductively coupled plasma optical emission spectrometer (ICP-OES) (Avio 500, PerkinElmer, United States). The ICP-OES was operated with a plasma power of 1,500 W, an argon plasma gas flow rate of 10 L/min, an auxiliary gas flow rate of 0.2 L/min, and a nebulizer gas flow rate of 0.6 L/min. Samples were pumped at a flow rate of 1.0 mL/min. Integration time for the measurements was set to 3 s with three replicates. The plasma view was set to radial for K, Ca, Mg, and Na, and axial for other elements. This setup ensured precise and accurate measurements of elemental concentrations in the bioreactor samples allowing for a comprehensive analysis of the correlation between water quality and the functionality of the Thiopaq system.

In order to evaluate the suitability of air injection into the bioreactor, the levels of SO_4^{2-}, chemical oxygen demand using dichromate (COD_{cr}), and total nitrogen (TN) in the solution were measured once a week using a spectrophotometer (DR6000, Hach, United States). Since the solution contained a significant amount of solid material, the solids were separated through centrifugation (5,000 *RCF*, 5 min) and a diluted sample of the supernatant was taken for measurement.

2.6 SOB community analysis

To further explore the correlation between bacterial diversity and Thiopaq system functionality, bioreactor samples were regularly collected from April 2022 to March 2023 with additional sampling during notable changes in the solution. DNA extraction was performed using the PowerMax Soil DNA Isolation Kit (Qiagen, Germany). The quantity of extracted DNA was measured using a fluorescence-based quantification technique with the QuantiFluor dsDNA System (Promega, United States) and the VICTOR Nivo Multimode Microplate Reader (PerkinElmer, United States) ensuring precise measurement. The quality of the extracted DNA was assessed by measuring the DNA Integrity Number (DIN) using the 2100 Bioanalyzer (Agilent Technologies, United States) which analyzed the distribution of signals of various sizes to determine the extent of DNA fragmentation. For long-read sequencing, the size distribution of DNA was verified using the Femto Pulse System (Agilent Technologies, United States).

Validated DNA samples were prepared into libraries following the Illumina 16S Metagenomic Sequencing Library protocol. The 16S ribosomal RNA (rRNA) was targeted with the V3-V4 region selected as the target region for phylogenetic classification (Fadeev et al., 2021; Bose and Moore, 2023; López-Aladid et al., 2023; Paul, 2023). The V3-V4 region of the 16S rRNA gene is widely used for species classification in bacterial studies due to its high variability which provides distinct genetic signatures for different species (Figure 3). It is flanked by conserved regions enabling the design of universal primers for broad amplification across bacterial species. With an optimal length of approximately 400–500 base pairs (bp), it is suitable for high-throughput sequencing platforms offering good coverage and taxonomic resolution. Additionally, extensive reference data in public databases support accurate microbial classification making the V3-V4 region a preferred choice in microbial taxonomy and metagenomics research. The selected samples were randomly fragmented and connected to $5'$ and $3'$ adapters through tagmentation. Adapter-ligated fragments were PCR amplified using a PCR primer solution matching the ends of the adapters. The first PCR products were purified using AMPure Beads (Beckman Coulter, United States), and libraries were constructed by attaching barcodes using the Nextera XT Index Kit (Illumina, United States) via a secondary PCR method. The size of the PCR-enriched fragments was confirmed using the DNA 1000 chip on the 2,100 Bioanalyzer. Accurate quantification of prepared libraries was performed using qPCR according to the Illumina qPCR Quantification Protocol Guide, ensuring optimal cluster density across the flow cell lane.

The validated final library templates were loaded onto the Illumina MiSeq system (Illumina, United States). Library fragments were captured on the complementary surface of adapter-bound oligos and each fragment was amplified into

TABLE 3 Average daily values of the operational parameters.

Sample	LFG						Thiopaq					
	CH$_4$ (%)	CO$_2$ (%)	O$_2$ (%)	LFG temperature (°C)	H$_2$S$_{in}$ (ppm)	H$_2$S$_{out}$ (ppm)	pH	ORP (mV)	Alkalinity (mEq/L)	Conductivity (mS/cm)	Imhoff reactor (mL/L)	Temperature reactor solution (°C)
Apr 2022	39.1	31.7	1.3	26.3	2,662	53	8.3	−326	660	52.1	34	28.2
May 2022	38.0	31.2	1.2	30.5	2,402	83	8.2	−334	680	52.7	30	29.6
Jun 2022	37.6	31.8	1.4	32.4	2,455	71	8.1	−357	680	53.8	36	30.4
Jul 2022	40.5	31.5	1.2	35.7	2,945	63	8.3	−366	680	53.5	25	32.0
Aug 2022	41.3	31.5	1.2	35.4	2,515	39	8.4	−375	820	54.4	30	31.5
Sep 2022	41.1	30.7	1.4	32.1	2,798	74	8.3	−391	790	54.3	30	30.7
Oct 2022	41.6	31.0	1.4	32.1	3,547	94	8.3	−393	770	54.1	31	30.6
Oct 2022 (u)	43.2	31.5	1.3	32.7	3,100	131	8.3	−375	650	51.7	0	30.8
Nov 2022 (u)	42.3	31.2	1.3	29.0	3,481	92	8.2	−367	700	52.5	0	32.3
Dec 2022 (u)	46.8	31.9	1.7	20.5	3,650	100	8.2	−355	680	48.9	0	28.8
Dec 2022	41.6	29.3	1.9	19.1	3,510	59	8.2	−350	650	48.6	45	24.6
Jan 2023	42.7	30.1	1.9	16.7	3,634	85	8.1	−325	650	48.2	47	22.8
Feb 2023	42.9	27.9	1.9	14.8	3,466	60	8.2	−284	590	48.2	38	20.6
Mar 2023 (u)	44.6	31.9	1.2	18.9	3,123	51	8.2	−298	550	47.9	11	23.6
Mar 2023	46.6	33.5	1.1	22.2	3,753	57	8.4	−313	570	51.3	50	26.9

individual clone clusters through bridge amplification. The Illumina sequencing-by-synthesis (SBS) technology utilized a reversible terminator-based method for detecting single bases inserted into the DNA template strand. After sequencing, raw images were processed using Illumina Real Time Analysis (RTA) software for system control and base calling. BCL (base call) binary files were converted to FASTQ files using the bcl2fastq software package provided by Illumina. The final paired-end sequencing data (2 × 300 bp) were analyzed for community diversity using species information and read counts obtained from the National Center for Biotechnology Information (NCBI) 16S database. This allowed for the investigation of microbial diversity and functionality within the Thiopaq system.

2.7 Scanning electron microscopy analysis of bio-sulfur

To investigate the surface morphology, scanning electron microscopy (SEM) analysis was performed on bio-sulfur particles. S^0 samples were collected by centrifugation (VS-5500, Vision, Bucheon, Korea) at 5,000 RCF for 5 min. The separated S^0 samples were then dehydrated at 65°C on a heat block (DRB200, Hach, United States) for 3 days. The dried bio-sulfur particles were mounted on an aluminum stub (Electron Microscopy Sciences, United States) using copper conductive double-sided tape (Ted Pella, United States) and coated with gold using an ion sputter (MC1000, Hitachi, Japan). The surface morphologies were observed using a high-resolution SU8230 field emission scanning electron microscope (FE-SEM, Hitachi, Japan) and a Zeiss Sigma 500 VP (FE-SEM, Carl Zeiss, Germany). Additionally, energy-dispersive X-ray spectroscopy (EDS), an accessory of the SU8230 FE-SEM, was utilized to analyze the surface elemental composition.

3 Results

3.1 Operational status

At the DBSL site, captured LFG was primarily supplied to the HWB for heat production. In cases of unavoidable circumstances, LFG was incinerated on-site for odor control purposes. Daesung Eco-energy operated a Thiopaq system to purify H_2S within the captured LFG at the DBSL site. An annual average of 3,028 ppm of H_2S was removed and the removal efficiencies were recorded at over 96% with an annual average of 97.5%. The inflow LFG temperature rose to a maximum of 36.2°C during the summer, while it dropped to a minimum of 14.4°C in the winter. Table 3 presents the average daily data for essential indicators, crucial for maintaining the growth conditions of the SOBs in the bioreactor, for each sampling day. These parameters are either continuously monitored and recorded in real-time [LFG data, H_2S, pH, oxidation-reduction potential (ORP), conductivity, and temperature], or measured and recorded every 4 hours (alkalinity and Imhoff).

The pH values were maintained between 8 and 9 with an annual average of 8.25. The target range for alkalinity was set between 550 and 800 mEq/L and the annual average value was 680 mEq/L. The conductivity levels were maintained between 45 and 60 mS/cm with an annual average value of 51.7 mS/cm. Additionally, Imhoff

reading values were measured in the bioreactor and settler with average values of 30 and 142, respectively.

However, in October, November, December 2022, and March 2023, there were instances where S^0 precipitates did not form properly within an hour resulting in no Imhoff value readings. Nevertheless, when the bioreactor solutions were left undisturbed for more than a day, viscous S^0 masses settled at the bottom of the Imhoff cone. These viscous S^0 masses could not be easily removed even by rinsing with water. These sampling points were defined as the unhealthy group (u), while other sampling points under normal operation conditions were categorized as the healthy group (Rouhollahi et al., 2024).

Unhealthy conditions in the Thiopaq system were observed whenever major installations of large-scale LFG extraction wells were completed at the DBSL site, as depicted in Figure 4. Although small-scale LFG extraction well installation and maintenance were ongoing throughout the year at the landfill site, unhealthy conditions did not occur. The unhealthy conditions typically occurred when all the LFG transfer pipeline valves were opened simultaneously, immediately after the completion of the large-scale LFG extraction well installations. As shown in Figures 2A–C, under unhealthy conditions, bio-sulfur became sticky and clumped together, and sulfur solidification caused severe blockages in the Thiopaq scrubber, leading to a differential pressure between the inlet (lower) and outlet (upper) sections.

If there is a malfunction in the decanter, the effective separation and discharge of substances such as sulfur dioxide (SO_2), H_2S, and sulfide ions (HS^-) from the solution are hindered leading to their accumulation over an extended period. This resulted in a rapid and substantial increase in COD_{cr} (exceeding 15,000 mg/L) accompanied by a rise in the foam level (with an Imhoff value of approximately 150 mL/L). The foam level continued to increase, but the ORP values began to decrease sharply at a certain point (data not shown). Attempts to increase ORP values by injecting more air resulted in the formation of a sludge-like foam causing overflow from the bioreactor as depicted in Figures 2D–F. After 1 to 2 hours of overflow, the foam gradually subsided. However, the foam that had previously accumulated on the surface of the bioreactor solution was not easily removed even when water was sprayed. Despite multiple occurrences, this phenomenon ceased when the LFG inflow rate was reduced and a substantial amount of the bioreactor solution was discharged and diluted.

3.2 Water quality analysis

For water quality analysis of the Thiopaq solution, monthly sampling was conducted. Additional sampling and analysis were also carried out when the S^0 in the solution was not properly formed and the SOB communities appeared unusual. Table 4 presents the measured values of the analyzed elements, although certain elements (Sr, Fe, Co, Cu, Mn, Zn, Mo, etc.) were not detected in this analysis.

3.3 SOB community analysis

To analyze the microbial community in the Thiopaq solution, monthly sampling was conducted. Additional sampling and analysis
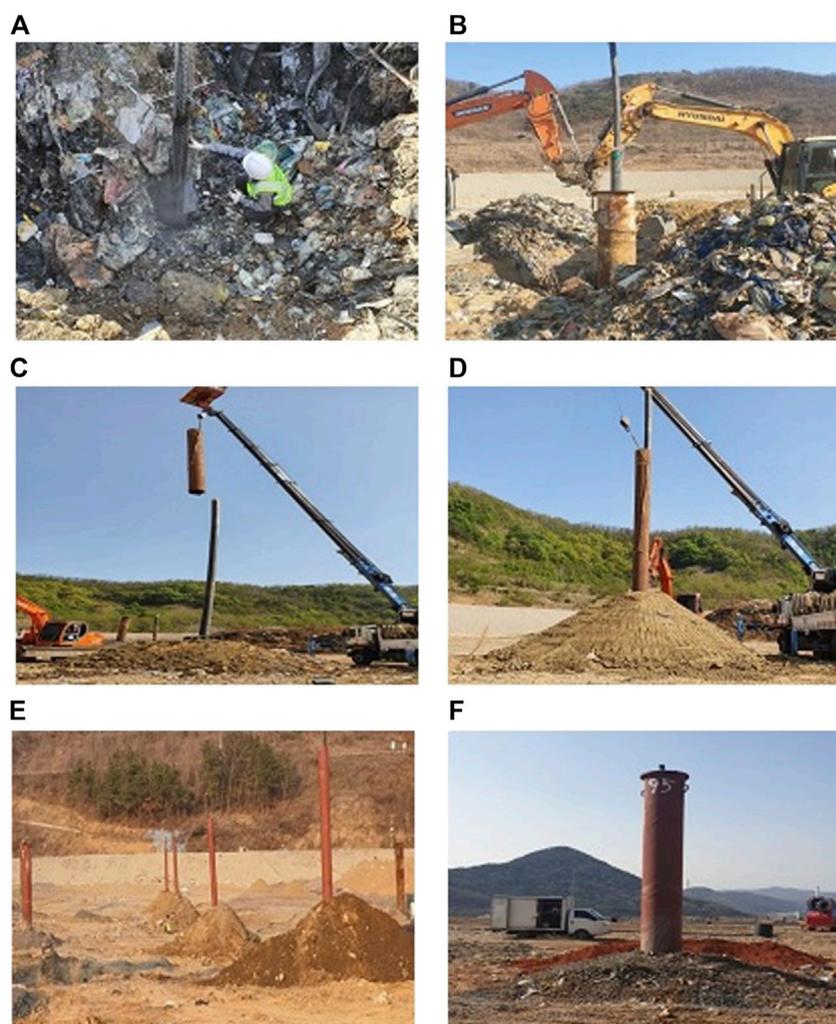
FIGURE 4
Installation process of an LFG extraction well: **(A)** construction site for the extraction well; **(B–D)** installation of the vertical extraction well; **(E, F)** completed LFG extraction wells.

were performed when the S^0 in the solution did not form properly and the SOB communities appeared abnormal. Figure 5A illustrates the relative abundance of the microbial community composition (above 1%). Figure 5B provides the maximum, minimum, and average ratios of the SOBs (above 1%). Additionally, Figure 5C depicts the richness and diversity of microbial communities within each sample.

Throughout the sampling duration, the most dominant species in the SOB community included *Thioalkalibacter halophilus*, *Alkalilimnicola ehrlichii*, and *Halothiobacillus kellyi*. All these species belong to the order Chromatiales. *T. halophilus* is part of the Thioalkalibacteraceae family, *A. ehrlichii* is a member of the Ectothiorhodospiraceae family, and *H. kellyi* belongs to the Halothiobacillaceae family. Initially, *T. halophilus* and *A. ehrlichii* were the two most predominant species. *T. halophilus* maintained a significant presence throughout the sampling period with its abundance ranging from as high as 61.0% to as low as 12.0%. In contrast, the population of *A. ehrlichii* gradually declined dropping from an initial relative abundance of 29.5% to less than 1.0% toward

the end of the sampling period. *H. kellyi* emerged in December 2022 and became a prominent species in 2023. Initially constituting less than 1.0% of the population, its abundance increased to 54.2% by the latter half of the sampling period contrasting to the decline of *T. halophilus*.

3.4 SEM analysis of bio-sulfur

The surface characteristics of S^0 samples under both healthy and unhealthy conditions were examined using FE-SEM. Figure 6 displays the surface morphology of S^0 presenting SEM images at various magnifications to facilitate a comparison between the two conditions. Under healthy conditions, S^0 particles exhibited a surface characterized by uneven and granular protrusions (Figures 6A, C, E, G). Additionally, these particles were often observed in an aggregated state forming irregularly shaped S^0 particles. The sizes of the aggregated, S^0 particles mainly ranged between 3 and 15 μm. In contrast, S^0 particles from the unhealthy condition exhibited

TABLE 4 Water quality analysis results of the bioreactor solutions (mg/L).

Sample	K	Mg	Ca	Na	S	P	Si
Apr 2022	41.90	12.45	5.79	17,826.98	10,005.23	2.37	3.55
May 2022	58.67	13.93	4.61	18,292.70	4,568.91	3.65	2.90
Jun 2022	48.59	9.28	4.37	19,409.98	6,976.92	1.46	2.11
Jul 2022	51.86	8.83	3.64	19,844.35	4,908.61	1.51	2.62
Aug 2022	50.66	7.47	3.82	20,006.79	5,867.62	0.98	2.72
Sep 2022	47.09	6.35	2.04	17,101.54	10,719.98	0.82	2.93
Oct 2022	52.83	6.44	2.78	19,716.52	19,602.42	0.79	3.43
Oct 2022 (u)	55.85	8.26	4.43	16,769.37	12,584.07	1.60	2.16
Nov 2022 (u)	73.29	10.55	2.84	18,694.30	14,427.74	1.93	2.74
Dec 2022 (u)	141.75	32.05	5.03	12,824.62	2,067.43	23.01	3.73
Dec 2022	69.41	12.80	3.81	12,480.23	1,961.76	3.54	3.50
Jan_2023	73.68	12.99	5.26	12,566.86	1,846.38	3.01	4.49
Feb 2023	74.09	13.62	7.54	11,584.77	1,687.93	3.93	5.23
Mar 2023 (u)	82.69	16.55	11.16	10,584.93	1,361.57	7.85	6.00
Mar 2023	98.51	20.33	10.48	13,328.82	1,908.18	8.59	5.71

individual bipyramidal crystal structures with uneven undulations on their smooth surfaces (Figures 6B, D, F, H). The crystal sizes varied between 2 and 10 μm. Furthermore, the elemental composition of S^0 particles analyzed by EDS showed the following percentages in healthy conditions: C: 19.71%, O: 8.67%, Na: 2.27%, S: 69.35%. In unhealthy conditions, the composition changed to: C: 45.29%, O: 7.75%, Na: 1.30%, S: 45.66%. Samples from healthy conditions contained a higher sulfur percentage and a lower carbon percentage compared to those from unhealthy conditions.

4 Discussion

4.1 Optimal operational conditions

The optimal operating conditions were not consistently constant and varied over time, primarily influenced by factors such as the microbial community, LFG temperature, composition, flow rate, and landfill site conditions. Maintaining alkalinity in the range of 700–800 mEq/L, conductivity between 40 and 55 mS/cm, and pH within the range of 8–8.5 generally resulted in stable operations with H_2S removal efficiency exceeding 95%. These values are slightly below those reported in previous studies which were over 99.9% (Benschop et al., 2002; Cline et al., 2003; Abdel Hamid et al., 2024). However, considering the extremely high concentration of over 2,000 ppm H_2S and the scale of the study landfill site, an annual average of 97.5% H_2S removal efficiency can be considered a promising figure. In general, desulfurization efficiency is reported to improve under haloalkaline conditions (de Rink et al., 2019; Zhao et al., 2021; Cattaneo et al., 2023;

Gupta et al., 2024). Moreover, the temperatures of the reaction solution in the bioreactor fluctuated with the changing seasons, yet the system remained effective even when temperatures dropped as low as 20°C. The operational temperatures observed in this study ranged from 20°C to 35°C. The biological desulfurization systems offer significant advantages as they can be operated at ambient temperatures (Syed et al., 2006; Kiragosyan et al., 2019; Johnston et al., 2023; Abdel Hamid et al., 2024). These benefits include improved energy efficiency, enhanced safety, reduced capital costs, and decreased maintenance complexity compared to chemical desulfurization processes.

Determining the optimal volume of air injection and the appropriate ORP level involved analyzing sulfate (SO_4^{2-}) and COD_{cr} levels as well as monitoring color changes in the bioreactor solution. The recommended ORP range, typically between −200 and −400 mV, maintains a reductive environment conducive to converting sulfide ions into S^0. This range supports the activities of SOBs utilized in the Thiopaq process which are optimized for slightly reductive conditions (Kiragosyan et al., 2020; de Rink et al., 2023). Additionally, it helps avoid overly oxidative conditions that could inhibit the reduction of sulfates to sulfides and their subsequent conversion to sulfur. Insufficient air supply led to an increase in COD_{cr} values and a deeper yellow color in the solution indicating reduced oxidation efficiency. On the other hand, excessive air supply caused elevated sulfate levels and reverted the solution's color from yellow back to its original white. The Thiopaq system uses air, specifically oxygen, to facilitate the aerobic oxidation of H_2S into S^0 by SOBs (Benschop et al., 2002; Cline et al., 2003; Pudi et al., 2022; Chan et al., 2023). When the air supply is inadequate, oxygen levels drop, decreasing H_2S conversion to sulfur and increasing other metabolic processes. High COD_{cr} values indicate the oxygen needed to oxidize substances in water. Insufficient oxygen can lead to the accumulation of intermediate sulfur species such as polysulfides or thiosulfates which deepen the solution's yellow color. Controlling the air supply is crucial to balance H_2S oxidation and prevent over-oxidation to sulfates ensuring efficient system performance. Variations in LFG inflow increased SO_4^{2-} and COD_{cr} values, while adjusting the decanter flow or diluting the bioreactor solution reduced them. Stabilizing COD_{cr} and SO_4^{2-} values is essential for consistent operation with appropriate air injection and ORP levels determined by observing these values and the bioreactor solution's color.

Furthermore, based on a previous study (Gupta et al., 2022), both the halophilic SOB genus *Guyparkeria* and the heterotrophic SOB genus *Halomonas* were identified as indicators of inadequate desulfurization system performance associated with increased sulfate and thiosulfate concentrations. The presence of *Guyparkeria* and *Halomonas* in desulfurization systems often signals inadequate system performance which can be attributed to several key factors. A notable increase in these bacterial genera can indicate a shift toward more saline conditions that disrupt microbial balance and inhibit essential sulfur-converting microorganisms. Additionally, these bacteria may become more dominant under conditions that cause the sulfur cycle to falter, such as when sulfates and thiosulfates do not convert fully,

FIGURE 5
Microbial community analysis in the bioreactor of the Thiopaq system (over 1% are shown): **(A)** relative abundance of bacterial community composition; **(B)** maximum, minimum, and average ratios of SOBs; **(C)** microbial community richness and diversity.
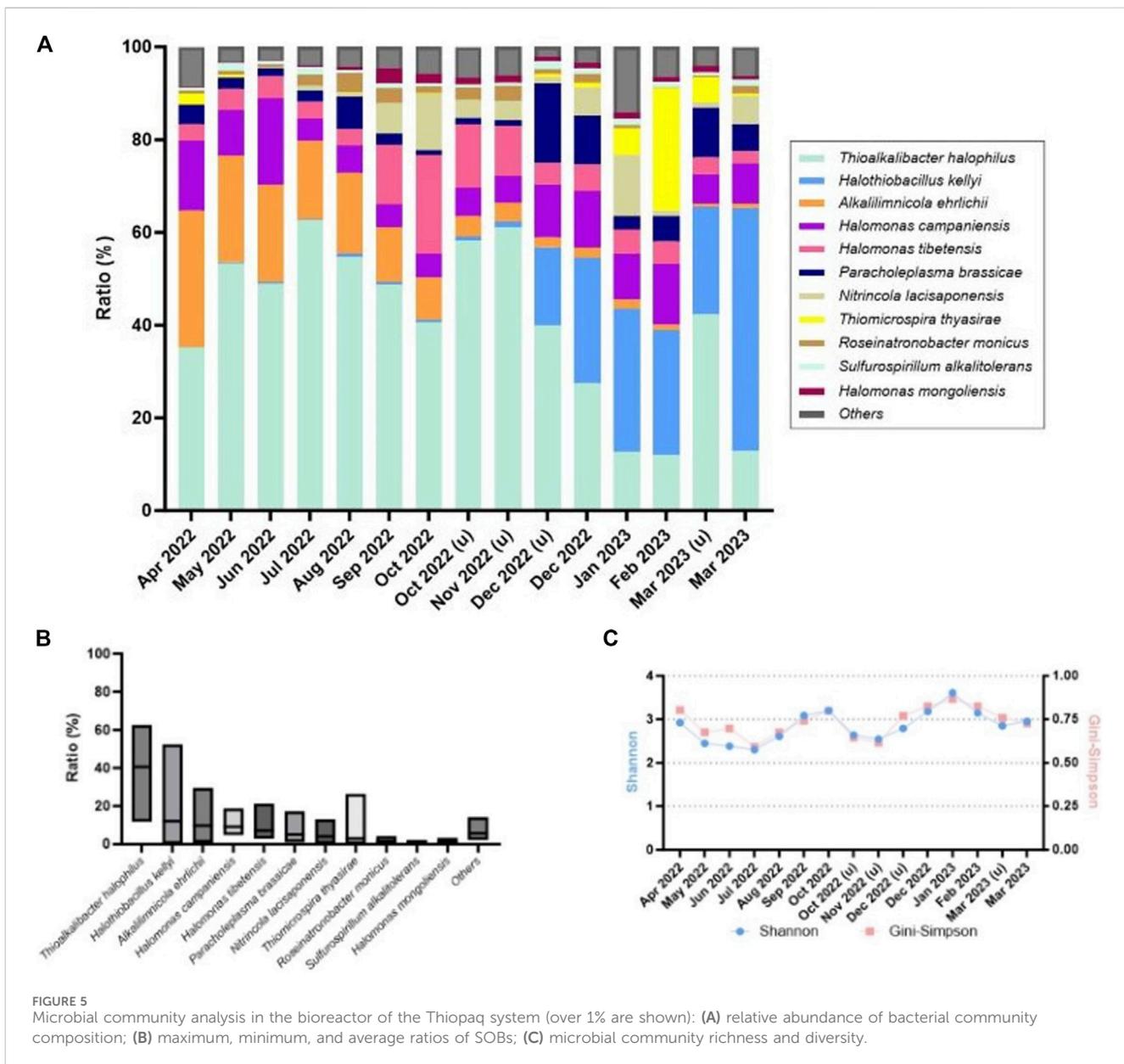
indicating process inefficiencies. Their proliferation might also reflect broader system stress, like nutrient imbalances, pH shifts, or fluctuating oxygen levels, which can impact overall desulfurization efficiency. Moreover, *Halomonas*, an obligate heterotroph that consumes organic matter and cannot use sulfide or thiosulfate as an energy source, may indicate excessive organic loads that the system fails to process efficiently (Sorokin et al., 2008). Analyzing operational data and changes in the SOB community in the Thiopaq system during this study revealed a positive correlation (R: 0.62) between the genus *Halomonas* and CODcr. Specifically, *H. tibetensis* exhibited a significantly positive correlation with CODcr (R: 0.88). Understanding the specific roles and conditions that favor *Guyparkeria* and *Halomonas* is crucial for diagnosing underlying issues and guiding adjustments to optimize system performance. Therefore, changes in the SOB community could serve as indicators for maintaining optimal operational conditions in the biodesulfurization system (Table 5).

4.2 Foam formation and overflow issues

In the biological removal of H_2S, rapid foam formation is a commonly observed challenge. According to previous research (Kleinjan et al., 2006), foam generation is influenced by factors such as gas flow rate, S^0 concentration, particle size distribution, and the presence of organic components. Two types of foam have been identified: unstable foam with small bubbles at low S^0 concentrations and stable foam with a polyhedral structure at high S^0 concentrations. The transition occurs when the local S^0 concentration near the surface exceeds a critical level leading to the formation of a stabilized film that prevents bubble bursting. This process results in increased bubble coalescence forming large bubbles, lamellae, and films which cause a rapid rise in foam height.

The foam phenomenon observed in Figures 2C–E resembles the stable foam described in the literature (Kleinjan et al., 2006). Imhoff
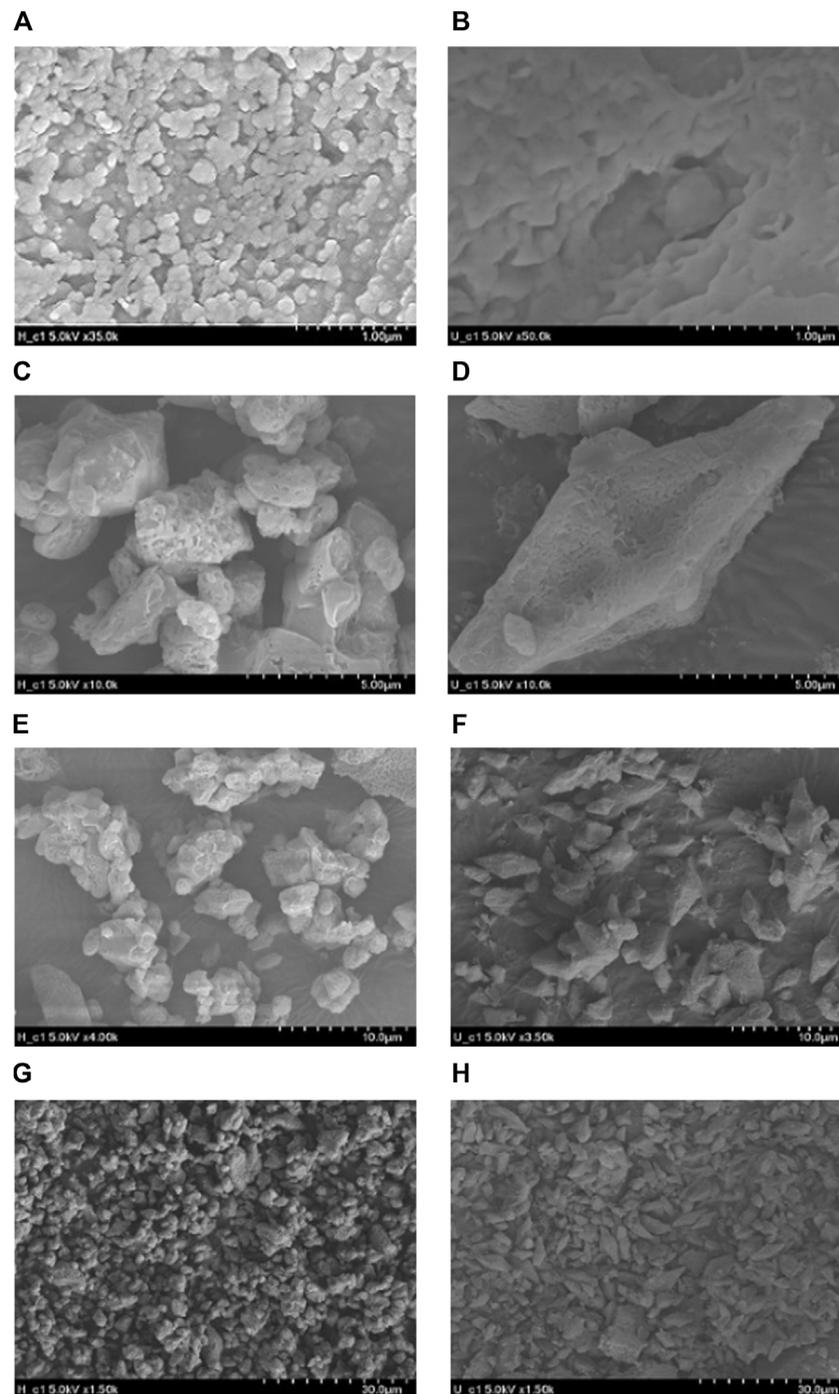
FIGURE 6
FE-SEM images of S^0 particles: scale bars **(A, B)** 1 μm; **(C, D)** 5 μm; **(E, F)** 10 μm; **(G, H)** 30 μm.

values exceeding 150 mL/L, coupled with decanter malfunction and a sharp increase in COD_{cr}, suggest a substantial presence of S^0 content and organic matter accumulation in the bioreactor solution.

The decanter, serving as a centrifuge separator, plays an important role in the Thiopaq system by using gravitational force to separate and remove S^0 particles from the solution, subsequently discharging the clarified solution back into the bioreactor (de Rink et al., 2019; de Rink et al., 2020). This process not only prevents the

accumulation of S^0 particles but also facilitates the regeneration of chemicals in the solution. However, when the decanter malfunctioned, its ability to effectively remove sulfur particles was compromised. This malfunction resulted in the buildup of S^0 content within the solution impeding the oxidation process of S^0 by SOBs. Consequently, the efficiency of SOB oxidation was hindered exacerbating the accumulation of organic matter and contributing to foam formation.

TABLE 5 Results of SO_4^{2-}, COD_{cr}, and TN measurements in the bioreactor solution.

Sample	Apr 2022	May 2022	Jun 2022	Jul 2022	Aug 2022
SO_4^{2-} (mg/L)	2,760	5,080	9,050	9,800	8,550
COD_{cr} (mg/L)	4,610	2,720	3,170	2,190	2,960
TN (mg/L)	105	73	226	271	314
Sample	Sep 2022	Oct 2022	Oct 2022 (u)	Nov 2022 (u)	Dec 2022 (u)
SO_4^{2-} (mg/L)	7,860	8,910	14,250	15,810	8,390
COD_{cr} (mg/L)	5,470	8,500	8,760	6,390	1,680
TN (mg/L)	347	303	206	178	298
Sample	Dec 2022	Jan 2023	Feb 2023	Mar 2023 (u)	Mar 2023
SO_4^{2-} (mg/L)	5,420	6,410	7,120	7,050	6,900
COD_{cr} (mg/L)	2,320	1,840	1,780	2,010	2,710
TN (mg/L)	75	74	89	126	128

To mitigate these issues, regular maintenance and monitoring of the decanter are essential. By ensuring the proper functioning of the decanter, S^0 particle discharge can be maintained at optimal levels, thereby preserving the integrity of the system and promoting efficient S^0 oxidation by SOBs. Additionally, maintaining operating conditions within specified thresholds for Imhoff values and COD_{cr} is crucial for preventing foam formation and organic matter accumulation ultimately enhancing the stability and performance of the system.

4.3 S^0 clogging issues

S^0 clogging is among the most encountered issues in the bio-desulfurization facility at the LFG facility. This phenomenon was also observed in the Thiopaq system at the DBSL site causing serious problems mainly in the interiors of the scrubber as shown in Figures 2A, B. It was reported that the desulfurization process of biogas containing thiols can lead to S^0 clogging (Chen et al., 2023). Thiols are compounds that possess a sulfhydryl (−SH) functional group. Bio-sulfur is characterized by its hydrophilic nature making it easy to separate and recover S^0 from the desulfurization process. However, the introduction of methanethiol (or methyl mercaptan, MeSH, CH_3SH) into the process removes hydrophilic biological polymers from the generated S^0 surfaces potentially leading to severe clogging in the interior of the scrubber.

MeSH is primarily generated during the initial phases of anaerobic decomposition (Chen et al., 2017) and higher MeSH levels are typically found in active landfills compared to inactive ones. A previous report by Kim (2006) indicated elevated MeSH concentrations in newly established landfills compared to existing ones. Major contributors to odor-related challenges at the DBSL site were identified as MeSH and other volatile organic sulfur compounds in previous studies (Kim, 2006; Jeon, 2014). The continuous increase in H_2S concentration indicates a corresponding rise in thiol concentrations in the captured LFG.

The DBSL site, being an active landfill, receives a substantial daily influx of municipal waste and new LFG extraction wells are frequently constructed especially in recently filled areas. These areas are likely in the early stages of anaerobic decomposition suggesting that after new well construction, additional thiols may have been introduced to the desulfurization system.

At the DBSL site, MeSH levels were regularly monitored using a gas detector tube (Gastec, Japan) to validate previous findings (Kim, 2006; Jeon, 2014). Our results indicated that in the new extraction well, CH_4 concentrations ranged from approximately 50%–60% and MeSH was detected in the range of 10–70 ppm. However, it should be noted that the maximum detection limit of the MeSH tube is 70 ppm and the actual MeSH levels might have been higher. Additionally, MeSH was detected in the range of 0–5 ppm in the extraction well with CH_4 concentrations of 40%–45%, while MeSH was not detected in wells with less than 40% CH_4.

Moreover, according to previous research (Kiragosyan et al., 2020), the introduction of MeSH resulted in *T. halophilus* becoming the dominant species in the SOB community after a certain period accompanied by a decrease in the *A. ehrlichii* population. Other literature by Roman et al. (2016a) also indicates that elevated levels of MeSH and ethanethiol correspond to *T. halophilus* becoming the dominant species. Additionally, it was also noted that *H. kellyi* was vulnerable to the LFG that contains MeSH (Chen et al., 2023). Originally, the genus *Thioalkalibacter* was classified within the Gamma Proteobacteria group of *Halothiobacillus* based on the 16S rRNA phylogeny. Later, this group was reorganized into the family Thioalkalibacteraceae to accommodate *T. halophilus* (Sorokin et al., 2020). Therefore, it can be considered that *T. halophilus* and *H. kellyi* are closely related species.

Additionally, *T. halophilus* is an obligately aerobic chemolithoautotrophic bacterium that utilizes sulfide and thiosulfate as energy sources and its tolerance to both CO_2 and MeSH was also well documented (Sorokin et al., 2020). However, there is no publication indicating that *H. kellyi* is tolerant to MeSH. Based on these findings, it could be concluded that *T. halophilus* is likely to dominate, while *H. kellyi* is more vulnerable to MeSH in

desulfurization systems processing LFG with high concentrations of thiols.

According to previous publications (Roman et al., 2016b; Kiragosyan et al., 2020; Sorokin et al., 2020; Chen et al., 2023), the observed changes in the SOB community composition suggest that *T. halophilus* dominated due to the continuous introduction of thiols into the Thiopaq system from the landfill site (Figure 5A). The presence of thiols in the biodesulfurization system was caused by ongoing small-scale construction works in 2022. During October, November, and December 2022, a significant amount of construction work was performed and these periods coincided with the periods in which the unhealthy conditions occurred. The dominance of *T. halophilus* and the decline in the *A. ehrlichii* population during these periods suggest that the introduction of high thiol concentrations contributed to the development of unhealthy conditions. However, from January 2023 onwards, the relative abundances of *H. kellyi* gradually increased. Considering the vulnerability of *H. kellyi* to MeSH, it could be inferred that the influx of thiols decreased from January.

To overcome the unhealthy conditions, a substantial amount of solution was discharged from the Thiopaq bioreactor starting from December 2022. This resulted in an increased input of chemicals. Additionally, the LFG temperatures significantly dropped during the winter months. These factors may have contributed to the dominance of *H. kellyi*. In March 2023, *T. halophilus* once again became the dominant species and the unhealthy conditions reoccurred. After recovery from the unhealthy condition, subsequent samples indicated the dominance of *H. kellyi* once again. These interpretations suggest a dynamic interplay between *T. halophilus* and *H. kellyi* influenced by changes in thiol compound concentrations and operational adjustments.

According to a prior study (Purwadi et al., 2023), it was observed that nutrients including PO_4^{3-} and Fe^{2+} influenced the formation and conversion rates of S^0 production. To investigate whether the unhealthy condition resulted from nutrient deficiencies, experiments were conducted in December 2022 by providing an excess of chemicals containing not only P and Fe but also other nutrient elements such as K and Mg. As a result, water quality analysis for the sample, Dec 2022 (u), in Table 4 showed significantly elevated levels of K, Mg, P, etc., with no detection of Fe. However, despite the increase in nutrient content in the bioreactor, the unhealthy condition was not resolved. This leads to the conclusion that the nutrient deficiency in the bioreactor solution was not the direct cause of the unhealthy condition.

Furthermore, in previous studies (Mol et al., 2020; Mol et al., 2021; Mol et al., 2022; Chen et al., 2023), SEM observations of bio-sulfur particles revealed a typical bipyramid crystal structure. In the SEM images presented in Figure 6, S^0 particles under unhealthy conditions appeared in a conventional bipyramid shape. However, the SEM images of the healthy condition exhibited a difference from the bipyramid shape revealing an irregularly aggregated form.

In the biological desulfurization process, the characteristics of S^0 particles play a crucial role. The continuous generation of small-sized S^0 particles reduces their sedimentation properties, making S^0 recovery challenging in desulfurization facilities and potentially causing operational issues (Mol et al., 2020; Mol et al., 2021). To address these challenges, various strategies have been explored to enhance sedimentation by promoting the aggregation of individual

S^0 particles (Mol et al., 2021). Biologically generated S^0 is enveloped in an organic coating composed of proteins and polysaccharides imparting hydrophilic properties (Marnocha et al., 2019). However, the introduction of thiol could remove these hydrophilic groups on the surface of S^0 particles (Chen et al., 2023).

According to Mol et al. (2022), a low sulfide-to-sulfur ratio limits the formation of polysulfides leading to the generation of relatively small S^0 crystals with insufficient sedimentation. This results in the accumulation of small S^0 particles. In the presence of thiol, these conditions create a vicious cycle where S^0 fails to separate effectively from the desulfurization facility causing a continuous formation of small S^0 particles with a decreasing sulfide-to-sulfur ratio. This unhealthy condition appears to be triggered by the introduction of thiol when the sulfide-to-sulfur ratio is low. Due to this ratio, the cohesion among sulfur particles is reduced resulting in smaller particles. Consequently, the introduction of thiol leads to the formation of small individual bipyramid S^0 crystals that do not sediment well and lose their hydrophilic properties leading to the accumulation of these crystals and the formation of sticky sulfur clusters that cause clogging. This observation is consistent with the state of S^0 particles in Figure 6 where unaggregated small individual bipyramid-shaped particles are evident under unhealthy conditions.

In the initial phase of our study, the potential impact of thiols on the bioreactor solution was not considered. Consequently, a comparative analysis of thiol contents in LFG before and after the installation of LFG extraction wells was not conducted. Future studies should focus on examining alterations in the microbial community concerning thiol levels in the LFG as well as investigating fluctuations in thiol concentrations before and after the construction of LFG extraction wells. Additionally, due to the extended duration of the installation work and varying collection pressure based on landfill conditions, it was challenging to determine the exact changes in flow rate. However, similar flow rates were achieved with reduced collection pressure and the LFG contained a higher CH_4 concentration after construction.

Furthermore, there were no effective methods for removing solidified sulfur inside the scrubber except for replacing the filling layer. This replacement is likely the most practical solution to address equipment clogging issues. Previous studies (Roman et al., 2016a; Mol et al., 2022; Chen et al., 2023) suggest that increasing the biomass of SOB and maintaining a higher sulfide concentration in the bioreactor could be effective in preventing S^0 clogging issues. Regularly discarding the bioreactor solution and/or enhancing the flow rate of the decanter to eliminate unstable small S^0 particles or other chemical by-products after new extraction well construction is another recommended precaution. Additionally, when opening valves in new extraction well construction areas, a gradual opening over several days is advised to avoid the sudden influx of thiol components. Ensuring an optimal growth environment for SOB by supplying sufficient nutrients is crucial for stable system operation.

4.4 Key findings and implications

In this study, the high efficiency of H_2S removal at the DBSL site using the Thiopaq system was demonstrated. The desulfurization process consistently achieved over 96% removal efficiency, with an

annual average of 97.5%, effectively reducing H_2S levels from the captured LFG. The successful operation was facilitated by maintaining essential parameters within optimal ranges such as a pH between 8 and 9, alkalinity between 550 and 800 mEq/L, and conductivity levels between 45 and 60 mS/cm. The stable performance under varying seasonal temperatures (14.4°C in winter to 36.2°C in summer) further highlights the robustness of the system in real-world conditions.

Operating parameters played a crucial role in ensuring the system's efficiency and stability. Maintaining the pH, alkalinity, and conductivity within target ranges, along with the control of ORP levels, contributed to the high H_2S removal efficiency. Regular monitoring and adjustments based on real-time data for these parameters were essential for preventing foam formation and ensuring effective bio-sulfur production. The study also identified the importance of avoiding sudden changes in LFG inflow rates and ensuring the proper functioning of the decanter to manage the system's stability and efficiency.

The production rate and purity of bio-sulfur were significantly influenced by the operating conditions and microbial community dynamics. Healthy conditions in the bioreactor were associated with the formation of irregularly aggregated S^0 particles with sizes ranging from 3 to 15 μm, whereas unhealthy conditions led to the production of smaller, bipyramidal S^0 crystals prone to causing blockages. The study highlighted the impact of thiol compounds, such as MeSH, on the microbial community composition and S^0 particle characteristics. The dominance of *T. halophilus* under high thiol conditions indicated the need for careful management of LFG composition to maintain optimal bio-sulfur production and prevent clogging issues.

Chemical consumption in the Thiopaq system was carefully managed to maintain optimal nutrient levels and ensure efficient S^0 production. The study revealed that nutrient deficiencies were not the primary cause of unhealthy conditions but rather the introduction of thiol compounds and their impact on microbial dynamics. Regular discharge of the bioreactor solution and controlled air injection rates were essential strategies to balance chemical consumption and maintain system performance. The findings underscore the importance of continuous monitoring, adaptive management, and preventive measures to sustain high desulfurization efficiency and bio-sulfur purity in landfill gas treatment processes.

4.5 Concluding remarks

This study provides a comprehensive overview of 1 year's operational data from the bio-desulfurization system at the DBSL highlighting observed changes in the microbial community under various conditions for the first time. These microbial community variations were identified as crucial indicators for analyzing the causes of diverse issues aiming to enhance our ability to address challenges in the bio-desulfurization process. Therefore, it is essential to implement

regular and long-term monitoring of the Thiopaq system's microbial community in alignment with the operational conditions at the DBSL. Factors such as landfill conditions, climate variations, and equipment malfunctions influence the community of SOB in the biological desulfurization process. Utilizing the SOB community as an indicator becomes crucial for detecting various issues and facilitating the maintenance of stable operations.

Data availability statement

The original contributions presented in the study are included in the article/Supplementary Material, further inquiries can be directed to the corresponding author.

Author contributions

EC: Conceptualization, Writing–original draft, Data curation, Formal Analysis, Investigation, Methodology, Software, Visualization. Y-HY: Data curation, Formal Analysis, Investigation, Methodology, Funding acquisition, Writing–review and editing. C-GB: Data curation, Investigation, Methodology, Software, Visualization, Writing–review and editing. JH: Conceptualization, Funding acquisition, Project administration, Supervision, Writing–original draft, Writing–review and editing, Validation.

Funding

Conflict of interest

The authors declare that the research was conducted in the absence of any commercial or financial relationships that could be construed as a potential conflict of interest.

Publisher's note

References

Abdel Hamid, M. F., Aboul-Fotouh, T. M., and El-Shafie, M. A. (2024). A comparison between Claus and THIOPAQ sulfur recovery techniques in natural gas plants. *J. Eng. Appl. Sci.* 71, 27. doi:10.1186/s44147-023-00356-9

Benschop, A., Janssen, A., Hoksberg, A., Seriwala, M., Abry, R., and Ngai, C. (2002). The Shell-Paques/THIOPAQ gas desulphurization process: successful start up first commercial unit. Available at: https://www.semanticscholar.org/paper/The-Shell-Paques-THIOPAQ-Gas-Desulphurisation-%3A-Up-Benschop-Janssen/4823edf767d9443d443c079b497c6747eaa730da.

Bose, N., and Moore, S. D. (2023). Variable region sequences influence 16S rRNA performance. *Microbiol. Spectr.* 11, e0125223. doi:10.1128/spectrum.01252-23

Cattaneo, C. R., Muñoz, R., Korshin, G. V., Naddeo, V., Belgiorno, V., and Zarra, T. (2023). Biological desulfurization of biogas: a comprehensive review on sulfide microbial metabolism and treatment biotechnologies. *Sci. Total Environ.* 893, 164689. doi:10.1016/j.scitotenv.2023.164689

Chan, Y. H., Loy, A. C. M., Cheah, K. W., Chai, S. Y. W., Ngu, L. H., How, B. S., et al. (2023). Hydrogen sulfide (H₂S) conversion to hydrogen (H₂) and value-added chemicals: progress, challenges and outlook. *Chem. Eng. J.* 458, 141398. doi:10.1016/j.cej.2023.141398

Chen, M., Yao, X. Z., Ma, R. C., Song, Q. C., Long, Y., and He, R. (2017). Methanethiol generation potential from anaerobic degradation of municipal solid waste in landfills. *Environ. Sci. Pollut. Res. Int.* 24, 23992–24001. doi:10.1007/s11356-017-0035-x

Chen, Z., Mu, T., Yang, M., Samak, N. A., Hao, X., Jia, Y., et al. (2023). Biologically produced elemental sulfur clogging induced by thiols in gas biodesulfurization systems. *Chem. Eng. J.* 462, 142196. doi:10.1016/j.cej.2023.142196

Chen, Z., Yang, G., Hao, X., Samak, N. A., Jia, Y., Peh, S., et al. (2021). Recent advances in microbial capture of hydrogen sulfide from sour gas via sulfur-oxidizing bacteria. *Eng. Life Sci.* 21, 693–708. doi:10.1002/elsc.202100006

Clean Air Conservation Act (2022). *Republic of Korea: national law information center.* Article 16.

Cline, C., Hoksberg, A., Abry, R., and Janssen, A. (2003). "Biological process for H₂S removal from gas streams: the Shell-Paques/THIOPAQ gas desulfurization process," in Proceedings of the Laurance Reid Gas Conditioning Conference, Norman (Oklahoma), USA, 23 –26 February 2003, 1–18.

de Rink, R., Klok, J. B. M., van Heeringen, G. J., Keesman, K. J., Janssen, A. J. H., Ter Heijne, A., et al. (2020). Biologically enhanced hydrogen sulfide absorption from sour gas under haloalkaline conditions. *J. Hazard. Mat.* 383, 121104. doi:10.1016/j.jhazmat.2019.121104

de Rink, R., Klok, J. B. M., van Heeringen, G. J., Sorokin, D. Y., Ter Heijne, A., Zeijlmaker, R., et al. (2019). Increasing the selectivity for sulfur formation in biological gas desulfurization. *Environ. Sci. Technol.* 53, 4519–4527. doi:10.1021/acs.est.8b06749

de Rink, R., Liu, D., Ter Heijne, A., Buisman, C. J. N., and Klok, J. B. M. (2023). Bacteria determine the measured oxidation reduction potential in the biological gas desulfurization process. *ACS Sustain. Chem. Eng.* 11, 38–46. doi:10.1021/acssuschemeng.2c03241

Enforcement Decree of the Wastes Control Act (2022). *Republic of Korea: national law information center.* Article 7.

Erdirencelebi, D., and Kucukhemek, M. (2018). Control of hydrogen sulphide in full-scale anaerobic digesters using iron (III) chloride: performance, origin and effects. *Water sa.* 44, 176–183. doi:10.4314/wsa.v44i2.04

Eun, S., Reinhart, D. R., Cooper, C. D., Townsend, T. G., and Faour, A. (2007). Hydrogen sulfide flux measurements from construction and demolition debris (C&D) landfills. *Waste Manage* 27, 220–227. doi:10.1016/j.wasman.2005.12.019

Fadeev, E., Cardozo-Mino, M. G., Rapp, J. Z., Bienhold, C., Salter, I., Salman-Carvalho, V., et al. (2021). Comparison of two 16S rRNA primers (V3-V4 and V4-V5) for studies of Arctic microbial communities. *Front. Microbiol.* 12, 637526. doi:10.3389/fmicb.2021.637526

Georgiadis, A. G., Charisiou, N. D., and Goula, M. A. (2020). Removal of hydrogen sulfide from various industrial gases: a review of the most promising adsorbing materials. *Catalysts* 10, 521. doi:10.3390/catal10050521

Gupta, S., de Rink, R., Klok, J. B. M., Muyzer, G., and Plugge, C. M. (2024). Process conditions affect microbial diversity and activity in a haloalkaline biodesulfurization system. *Appl. Environ. Microbiol.* 90, e0186423–23. doi:10.1128/aem.01864-23

Gupta, S., Plugge, C. M., Klok, J. B. M., and Muyzer, G. (2022). Comparative analysis of microbial communities from different full-scale haloalkaline biodesulfurization systems. *Appl. Microbiol. Biotechnol.* 106, 1759–1776. doi:10.1007/s00253-022-11771-y

Hou, N., Xia, Y., Wang, X., Liu, H., Liu, H., and Xun, L. (2018). H₂S biotreatment with sulfide-oxidizing heterotrophic bacteria. *Biodegradation* 29, 511–524. doi:10.1007/s10532-018-9849-6

Jeon, J. M. (2014). "Optimal management and reduction plan for odor generation from landfill (2012000160006)," in *Technologies for responding to atmospheric environment policies Korea environmental industry and technology Institute* (Ministry of Environment of Korea).

Johnston, K. A. K. Y., van Lankveld, M., de Rink, R., Roman, P., Klok, J. B. M., Mol, A. R., et al. (2023). Polysulfide concentration and chain length in the biological

desulfurization process: effect of biomass concentration and the sulfide loading rate. *Environ. Sci. Technol.* 57, 13530–13540. doi:10.1021/acs.est.3c03017

Kim, K. H. (2006). Emissions of reduced sulfur compounds (RSC) as a landfill gas (LFG): a comparative study of young and old landfill facilities. *Atmos. Environ.* 40, 6567–6578. doi:10.1016/j.atmosenv.2006.05.063

Kiragosyan, K., Klok, J. B. M., Keesman, K. J., Roman, P., and Janssen, A. J. H. (2019). Development and validation of a physiologically based kinetic model for starting up and operation of the biological gas desulfurization process under haloalkaline conditions. *Water Res. x.* 4, 100035. doi:10.1016/j.wroa.2019.100035

Kiragosyan, K., Picard, M., Timmers, P. H. A., Sorokin, D. Y., Klok, J. B. M., Roman, P., et al. (2020). Effect of methanethiol on process performance, selectivity and diversity of sulfur-oxidizing bacteria in a dual bioreactor gas biodesulfurization system. *J. Hazard. Mat.* 398, 123002. doi:10.1016/j.jhazmat.2020.123002

Kleinjan, W. E., de Keizer, A., and Janssen, A. J. H. (2003). Biologically produced sulfur. *Top. Curr. Chem.* 230, 167–188. doi:10.1007/b12114

Kleinjan, W. E., Marcelis, C. L. M., Keizer, A. D., Janssen, A. J. H., and Stuart, M. A. C. (2006). Foam formation in a biotechnological process for the removal of hydrogen sulfide from gas streams. *Colloids Surf. A Physicochem. Eng. Asp.* 275, 36–44. doi:10.1016/j.colsurfa.2005.09.015

Ko, J. H., Xu, Q., and Jang, Y. C. (2015). Emissions and control of hydrogen sulfide at landfills: a review. *Crit. Rev. Environ. Sci. Technol.* 45, 2043–2083. doi:10.1080/10643389.2015.1010427

Long, Y., Fang, Y., Shen, D., Feng, H., and Chen, T. (2016). Hydrogen sulfide (H₂S) emission control by aerobic sulfate reduction in landfill. *Sci. Rep.* 6, 38103. doi:10.1038/srep38103

López-Aladid, R., Fernández-Barat, L., Alcaraz-Serrano, V., Bueno-Freire, L., Vázquez, N., Pastor-Ibáñez, R., et al. (2023). Determining the most accurate 16S rRNA hypervariable region for taxonomic identification from respiratory samples. *Sci. Rep.* 13, 3974. doi:10.1038/s41598-023-30764-z

Marnocha, C. L., Sabanayagam, C. R., Modla, S., Powell, D. H., Henri, P. A., Steele, A. S., et al. (2019). Insights into the mineralogy and surface chemistry of extracellular biogenic S⁰ globules produced by *Chlorobaculum tepidum*. *Front. Microbiol.* 10, 271. doi:10.3389/fmicb.2019.00271

Mol, A. R., Langeveld, L. J. V., Weijden, R. D. V. D., Klok, J. B. M., and Buisman, C. J. N. (2022). Effect of sulfide on morphology and particle size of biologically produced elemental sulfur from industrial desulfurization reactors. *J. Hazard. Mat.* 424, 127696. doi:10.1016/j.jhazmat.2021.127696

Mol, A. R., Meuwissen, D. J. M., Pruim, S. D., Zhou, C., Vught, V. V., Klok, J. B. M., et al. (2021). Novel agglomeration strategy for elemental sulfur produced during biological gas desulfurization. *ACS Omega* 6 (42), 27913–27923. doi:10.1021/acsomega.1c03701

Mol, A. R., Weijden, R. D. V. D., Klok, J. B. M., and Buisman, C. J. N. (2020). Properties of sulfur particles formed in biodesulfurization of biogas. *Minerals* 10, 433. doi:10.3390/min10050433

Nam, S. C., Hur, K. B., and Lee, N. H. (2011). Effects of hydrogen sulfide and siloxane on landfill gas utility facilities. *Environ. Eng. Res.* 16, 159–164. doi:10.4491/eer.2011.16.3.159

Oh, S. J., Ha, S. H., Noh, E. J., Shin, S. G., and Ahn, J. H. (2024). Effect of iron powder on hydrogen sulfide reduction and phosphate removal in semi-continuous anaerobic digestion treating primary sludge. *J. Chem. Technol. Biotechnol.* 99, 893–901. doi:10.1002/jctb.7594

Panza, D., and Belgiorno, V. (2010). Hydrogen sulphide removal from landfill gas. *Process Saf. Environ. Prot.* 88, 420–424. doi:10.1016/j.psep.2010.07.003

Paul, B. (2023). Concatenated 16S rRNA sequence analysis improves bacterial taxonomy. *F1000Res* 11, 1530. doi:10.12688/f1000research.128320.3

Plaza, C., Xu, Q., Townsend, T., Bitton, G., and Booth, M. (2007). Evaluation of alternative landfill cover soils for attenuating hydrogen sulfide from construction and demolition (C&D) debris landfills. *J. Environ. Manage.* 84, 314–322. doi:10.1016/j.jenvman.2006.06.001

Pudi, A., Rezaei, M., Signorini, V., Andersson, M. P., Baschetti, M. G., and Mansouri, S. S. (2022). Hydrogen sulfide capture and removal technologies: a comprehensive review of recent developments and emerging trends. *Sep. Purif. Technol.* 298, 121448. doi:10.1016/j.seppur.2022.121448

Purwadi, R., Ginting, D. A. E. B., Anbibie, A., Mohtar, W. H. M. W., Ramli, Y., and Indarto, A. (2023). Effects of nutrients on the performance of the biological sulfur recovery unit for sulfur removal from water. *Water* 15, 530. doi:10.3390/w15030530

Roman, P., Klok, J. B. M., Sousa, J. A. B., Broman, E., Dopson, M., Zessen, E. V., et al. (2016a). Selection and application of sulfide oxidizing microorganisms able to withstand thiols in gas biodesulfurization systems. *Environ. Sci. Technol.* 50, 12808–12815. doi:10.1021/acs.est.6b04222

Roman, P., Lipińska, J., Bijmans, M. F. M., Sorokin, D. Y., Keesman, K. J., and Janssen, A. J. H. (2016b). Inhibition of a biological sulfide oxidation under haloalkaline

conditions by thiols and diorgano polysulfanes. *Water Res.* 101, 448–456. doi:10.1016/j.watres.2016.06.003

Rouhollahi, A. A., Giyahchi, M., Dastgheib, S. M. M., and Moghimi, H. (2024). Assessing the efficiency and microbial diversity of H2S-removing biotrickling filters at various pH conditions. *Microb. Cell Fact.* 23, 157. doi:10.1186/s12934-024-02427-9

Rujisangvittaya, K., and Phoolphundh, S. (2015). Sulfur oxidizing bacterial biofilter for removal of hydrogen sulfide (H$_2$S) from biogas. J. *Renew. Energy Environ.* 6, 71–74.

Sorokin, D. Y., Merkel, A. Y., and Muyzer, G. (2020). "Thioalkalibacter," in *Bergey's manual of systematics of archaea and bacteria.* Editor A. Oren (New York, USA: John Wiley and Sons Inc.), 1–6. doi:10.1002/9781118960608.gbm01692

Sorokin, D. Y., van den Bosch, P. L., Abbas, B., Janssen, A. J., and Muyzer, G. (2008). Microbiological analysis of the population of extremely haloalkaliphilic sulfur-oxidizing bacteria dominating in lab-scale sulfide-removing bioreactors. *Appl. Microbiol. Biotechnol.* 80, 965–975. doi:10.1007/s00253-008-1598-8

Syed, M., Soreanu, G., Falletta, P., and Béland, M. (2006). Removal of hydrogen sulfide from gas streams using biological processes – a review. *Can. Biosyst. Eng.* 48, 1–14.

Tolaymat, T., and Carson, D. (2015). *Best management practices to prevent and control hydrogen sulfide and reduced sulfur compound emissions at landfills that dispose of gypsum drywall (EPA/600/R-14/039).* Washington, DC, USA: U.S. Environmental Protection Agency.

Toledo-Cervantes, A., Lebrero, R., Cavinato, C., and Muñoz, R. (2017). "Biogas upgrading using algal-bacterial processes," in *Microalgae-based biofuels and bioproducts.* Editors G. -Fernandez and V. Raúl Muñoz (Woodhead Publishing Series in Energy), 283–304. doi:10.1016/B978-0-08-101023-5.00012-1

Vikrant, K., Kailasa, S. K., Tsang, D. C. W., Lee, S. S., Kumar, P., Giri, B. S., et al. (2018). Biofiltration of hydrogen sulfide: trends and challenges. *J. Clean. Prod.* 187, 131–147. doi:10.1016/j.jclepro.2018.03.188

Wang, C., Fang, X., Zhao, F., Deng, Y., Zhu, X., Deng, Y., et al. (2022). Effective removal of hydrogen sulfide from landfill gases using a modified iron pentacarbonyl desulfurization agent and the desulfurization mechanism. *Sci. Total Environ.* 839, 156160. doi:10.1016/j.scitotenv.2022.156160

Wastes Control Act (2023). *Republic of Korea: national law information center.* Article 2.

Zhao, Y., Wang, J., Liu, Y., Zheng, P., and Hu, B. (2021). Microbial interaction promotes desulfurization efficiency under high pH condition. *Environ. Res.* 200, 111423. doi:10.1016/j.envres.2021.111423